Progress In Electromagnetics Research Letters, Vol. 37, 91–99, 2013

DUAL-BAND COUPLING ELEMENT BASED ANTENNAS WITH HIGH PORT ISOLATION

Wen Jiang*, Tao Hong, and Chao Li

National Key Laboratory of Antennas and Microwave Technology, Xidian University, Xi'an, Shaanxi 710071, P. R. China

Abstract—A compact dual-band MIMO coupling element based antenna with high port isolation is proposed for the first time. The proposed antenna comprises four nonresonant coupling elements, the matching circuit, chassis of the mobile terminal, and de-coupling structures. The proposed antenna can cover two working bands of E-GSM900 and PCS1900. The measured results show that the isolation between the coupling elements operating at the same frequency is higher than 20 dB. The proposed structure can be applied to the MIMO system.

1. INTRODUCTION

Wireless communication systems should be capable of accommodating higher data rates. The use of multi-element antennas, such as multiple input multiple out (MIMO) antennas is one of the most effective ways to improve reliability and increase the channel capacity of communication systems [1, 2]. On the other hand, dual-band components are preferred as many popular communication systems operating in dual bands. At the same time, the demand for low-cost and portable electronic products calls for size miniaturization of the system [3, 4]. However, it is very difficult to integrate multiple antennas in a small and compact space while maintaining good isolation between antenna elements, especially for dual-band antenna arrays [5–14].

Papers [15, 16] presented comprehensive studies on coupling element based antenna structures for mobile communication terminals. The antenna was novel and useful for the future design of low-volume and low-profile antennas for portable terminals. Essentially nonresonant coupling elements were used to optimally couple to the

Received 18 December 2012, Accepted 11 January 2013, Scheduled 19 January 2013

* Corresponding author: Wen Jiang (jw13@vip.qq.com).

dominating characteristic wavemodes of the chassis, and the antenna structures were tuned to resonance with matching circuits. Hence, this kind of antennas is not suitable for MIMO systems.

In this paper, a novel low-profile dual-band MIMO antenna with high port isolation is presented. The designed dual-band antenna works by efficiently utilizing the radiation of the currents on the chassis ground which can reduce the volume of mobile terminal antenna elements [15]. In this paper to apply this antenna to MIMO systems, a dual-band de-coupling structure is used on the chassis ground. The de-coupling structure is placed on the edge of the chassis ground, which produces little effect on the placement of the other devices. The designed antenna basically consists of four nonresonant coupling elements, two matching circuitries, the chassis of the mobile terminal, and de-coupling structures. It operates at 0.9/1.9 GHz.

Firstly, two sets of nonresonant coupling elements are used to optimally couple to the dominating characteristic wavemodes of the chassis. And then, to achieve low mutual coupling between the two antenna elements, two sets of cross slots etched on the two edges of the ground are added. Finally, matching circuits are designed to obtain good impedance matching for the lower and upper bands. Measured results show that the proposed MIMO antenna has high port isolation while maintaining good impedance matching. Meanwhile, the antenna is compact in size, simple in structure and easy to fabricate.

2. ANTENNA DESIGN

The proposed dual-band MIMO antenna has four parts, shown in Fig. 1. The four parts are nonresonant coupling elements, two matching circuitries, a chassis ground of the mobile terminal, and two de-coupling structures. The mobile terminal chassis is meant to work as the main radiator of the antenna structure. The size of the chassis ground are not strict and should be designed according to the terminal device. In this paper, a $W \times L = 60\,\text{mm} \times 100\,\text{mm}$ substrate is used.

To achieve sufficient impedance bandwidth, the dominant wavemode of the chassis has to be excited somehow. For this purpose, the nonresonant coupling elements are used. Coupling to the chassis wavemode can be done either via the magnetic or the electric fields of the chassis wavemodes. A plate or probe can be arranged so that its electric field direction is parallel to that of the chassis wavemode. The modularity of the structure enables the use of separate coupling elements. And the coupling element does not need to be tuned to resonance, extremely compact coupling elements can be used even at very low frequencies without the need of meandering. Hence in this

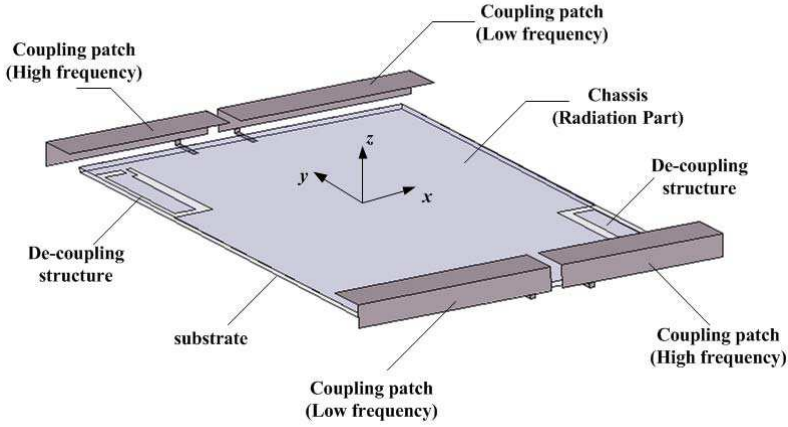

Figure 1. Geometry of the proposed antenna structure.

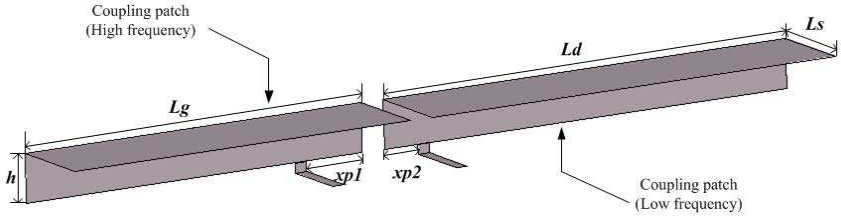

Figure 2. Geometry of the nonresonant coupling elements.

paper, four nonresonant coupling elements are designed for high and low frequency coupling patches. The two coupling patches with a same working frequency are placed in diagonal line position of the substrate. In order to couple strongly to the chassis dominant wavemode, the location and shape of the coupling element have to be chosen correctly. The effect of the coupling element location on the achievable radiation quality factor should be studied and the sizes of the coupling element will be located optimally and determined by using HFSS 12.0. The sizes are shown: $L_g = 30\,\text{mm}$, $L_d = 34\,\text{mm}$, $L_s = 8\,\text{mm}$, $xp_1 = 5\,\text{mm}$, $h = 4\,\text{mm}$. They are shown in Fig. 2.

The de-coupling structures and matching circuit are integrated on the bottom and top portions of a grounded FR4 substrate with

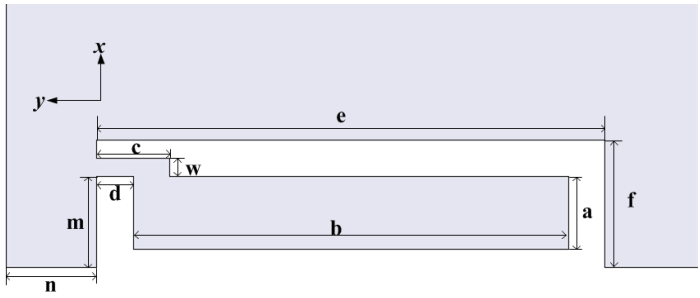

Figure 3. Geometry of the de-coupling structure.

a thickness of 0.8 mm and relative permittivity of 4.4, separately. The total dimension of the substrate is $W \times L = 60\,\text{mm} \times 100\,\text{mm}$. To decrease the mutual coupling, the de-coupling structures are introduced and shown in Fig. 3.

By using the EM simulator HFSS_V12, the optimized dimensions are: $n = 5\,\text{mm}$, $m = 5\,\text{mm}$, $b = 24\,\text{mm}$, $a = 4\,\text{mm}$, $c = 4\,\text{mm}$, $w = 1\,\text{mm}$, $d = 2\,\text{mm}$, $e = 28\,\text{mm}$, $f = 7\,\text{mm}$. The surface current on the chassis ground with or without de-coupling structure is shown in Fig. 4. As shown in Fig. 4, the surface current is controlled well after adding the proposed de-coupling structures at the two bands. However, the introduced structures would greatly change the input impedances. Hence, the four nonresonant coupling elements should be connected with the matching circuits. The topologies of the matching circuit is shown in Fig. 5. The optimized parameters are as follow: $C_1 = 1\,\text{pF}$, $L_1 = 22.6\,\text{nH}$, $L_2 = 7.5\,\text{nH}$, $L_3 = 6.2\,\text{nH}$, $C_2 = 1\,\text{pF}$, $L_4 = 3.2\,\text{nH}$, $L_5 = 2.7\,\text{nH}$, $C_3 = 1.4\,\text{pF}$.

3. RESULTS AND DISCUSSIONS

The proposed dual-band MIMO antenna is fabricated and measured. Measured S-parameters of the proposed antenna are shown in Fig. 6. Since the four antennas are symmetric, only $|S_{11}|$, $|S_{21}|$, $|S_{33}|$, and $|S_{43}|$ are given. Ports 1 and 2 correspond to the low frequency, while Ports 3 and 4 to the high frequency.

It can be clearly observed that the measured impedance bandwidths are 0.86 to 0.93 GHz and 1.84 to 1.99 GHz. The measured isolation is higher than 20 dB in both the lower and upper bands, indicating a good MIMO performance of the structure. The maximum isolation is nearly 20.3 dB at 0.9 GHz and 22.5 dB at 1.9 GHz.

The measured radiation patterns of the designed high-isolation

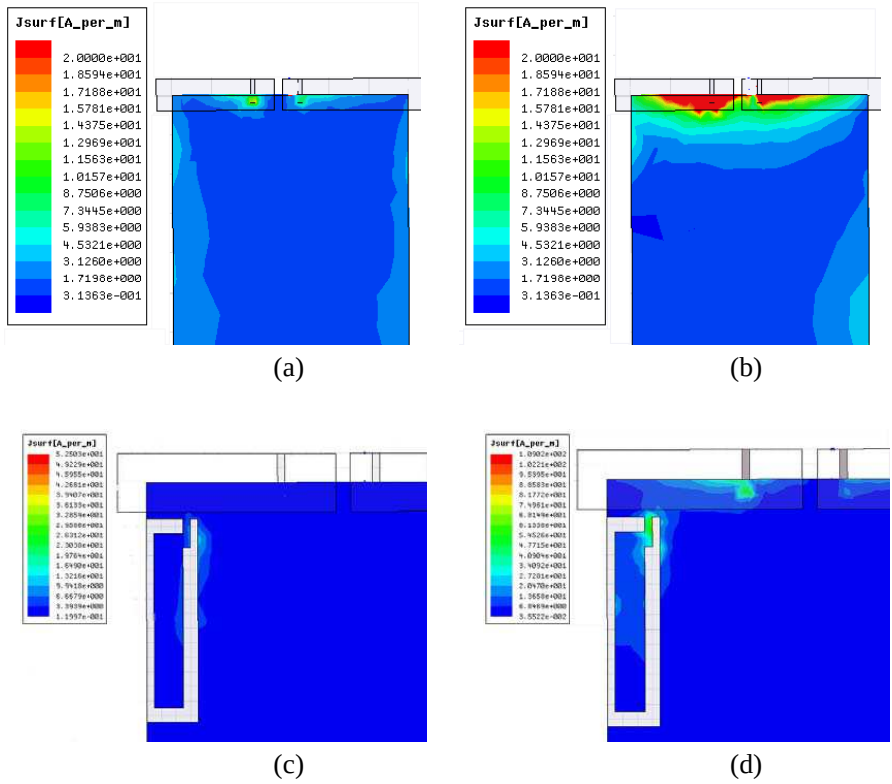

Figure 4. Surface current on the chassis ground. (a) 0.9 GHz, without de-coupling structure. (b) 1.9 GHz, without de-coupling structure. (c) 0.9 GHz, with de-coupling structure. (d) 1.9 GHz, with de-coupling structure.

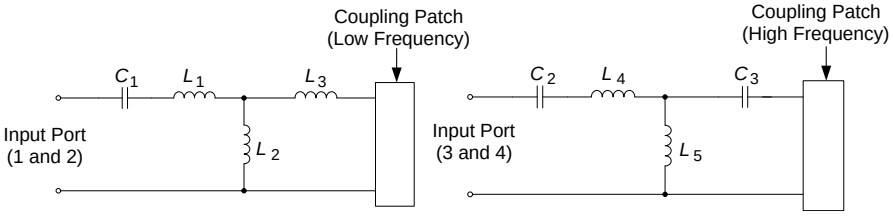

Figure 5. The topologies of the matching circuit.

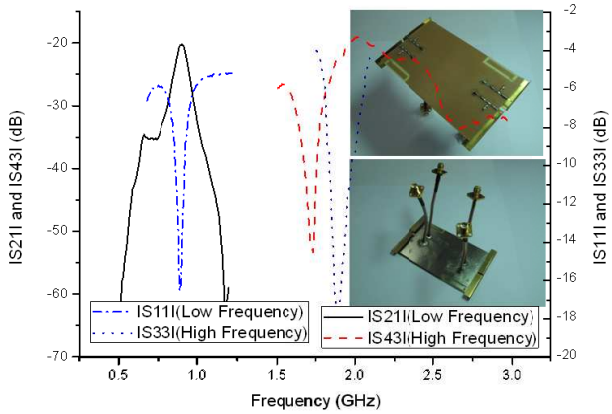

Figure 6. Measured S-parameters of proposed antenna.

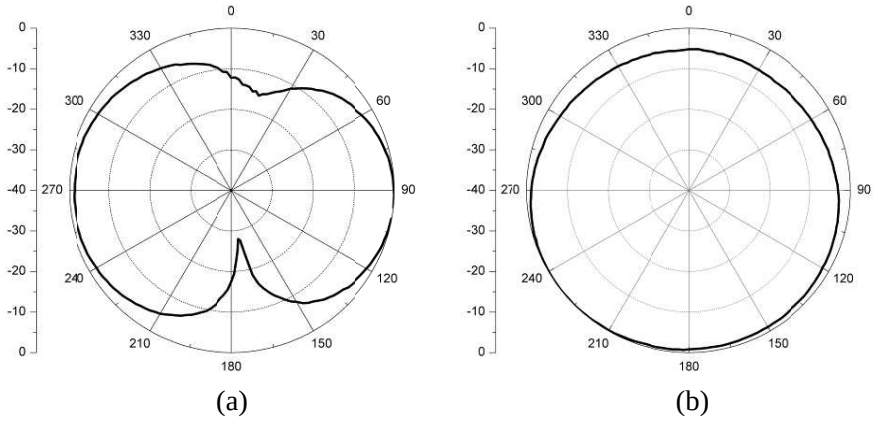

Figure 7. Measured radiation patterns at 0.9 GHz. (a) E-plane. (b) H-plane.

antenna at 0.9 and 1.9 GHz are given in Fig. 7 and Fig. 8, respectively, with port 1 or 3 excited and the other ports terminated to a 50 ohm load. The peak gain of the proposed antenna is 2.7 dBi at 0.9 GHz and 3.8 dBi at 1.9 GHz.

Envelope correlation coefficient (ECC) is an important parameter to the diversity gain of a MIMO system. Generally, low envelope correlation always leads to high diversity gain. For a two-antenna

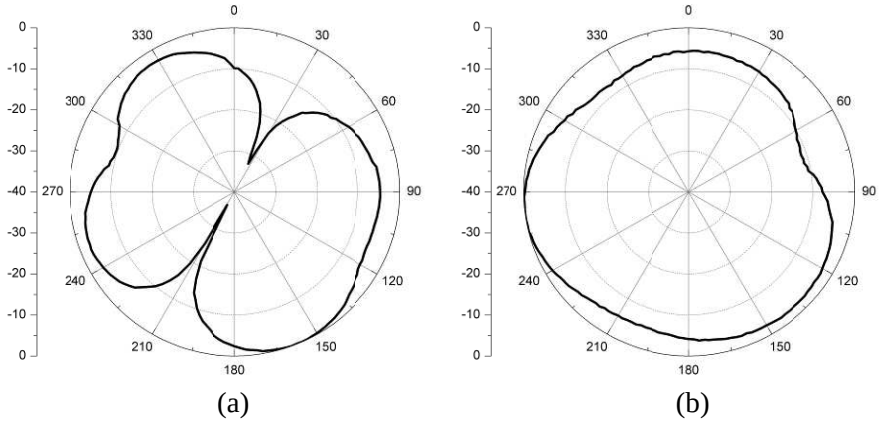

Figure 8. Measured radiation patterns at 1.9 GHz. (a) E-plane. (b) H-plane.

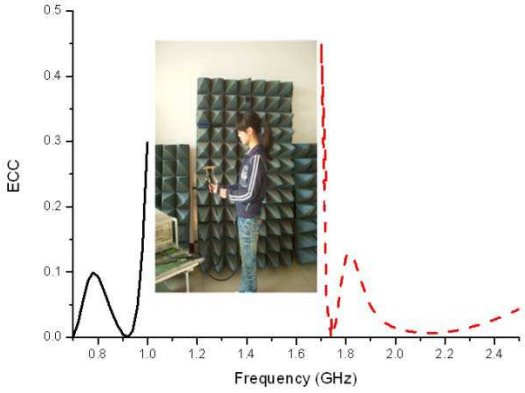

Figure 9. Calculated result of ECC.

system, we can use a simple formula to calculate ECC [16]:

$$\rho = \frac{\left|S_{11}^* S_{21} - S_{12}^* S_{22}\right|^2}{\left(1 - \left|S_{11}\right|^2 - \left|S_{21}\right|^2\right)\left(1 - \left|S_{22}\right|^2 - \left|S_{12}\right|^2\right)} \tag{1}$$

The calculated result of the proposed antenna is exhibited in Fig. 9. It shows that the desired operation bands of the proposed antenna have an ECC less than 0.1, which means that the antenna has good diversity gain.

4. CONCLUSION

In this paper, a compact dual-band MIMO antenna with high port isolation is proposed. The antenna consists of four nonresonant coupling elements, two matching circuitries, chassis of the mobile terminal, and de-coupling structures. The measured isolation is higher than 20 dB in both the lower and upper bands, indicating a good MIMO performance of the structure. Moreover, this antenna also shows low envelope correlation, which leads to good diversity gain. Conclusively, it is expected that the proposed structure can be applied to the MIMO system.

ACKNOWLEDGMENT

The authors would like to thank the financial support from the National Natural Science Fundation of China (No. 61201018). We are also especially grateful to Anechoic Chamber of National Laboratory of Antennas and Microwave Technology of China for providing measuring facilities.

REFERENCES

1. Gesbert, D., M. Shafi, D. S. Shiu, P. Smith, and A. Naguib, "From theory to practice: An overview of MIMO space-time coded wireless systems," *IEEE Journal on Selected Areas in Communications*, Vol. 21, No. 3, 281–302, 2003.
2. Cui, S., Y. Liu, W. Jiang, and S. X. Gong, "Compact dual-band monopole antennas with high port isolation," *Electronics Letters*, Vol. 47, No. 10, 579–580, 2011.
3. Jensen, M. A. and J. W. Wallace, "A review of antennas and propagation for MIMO wireless communications," *IEEE Transactions on Antennas and Propagation*, Vol. 52, No. 11, 2810–2824, 2004.
4. Gong, Q., Y.-C. Jiao, and S.-X. Gong, "Compact MIMO antennas using a ring hybrid for WLAN applications," *Journal of Electromagnetic Waves and Applications*, Vol. 25, Nos. 2–3, 431–441, 2011.
5. Li, H., J. Xiong, and S. L. He, "Extremely compact dual-band PIFAs for MIMO application," *Electronics Letters*, Vol. 45, No. 17, 869–870, 2009.
6. Jusoh, M., M. F. B. Jamlos, M. R. B. Kamarudin, and M. F. B. A. Malek, "A MIMO antenna design challenges for UWB

application," *Progress In Electromagnetics Research B*, Vol. 36, 357–371, 2012.

7. Bae, S., Y.-K. Hong, J.-J. Lee, J.-H. Park, J. Jalli, G. Abo, H. M. Kwon, and C. K. K. Jayasooriya, "Miniature and higher-order mode ferrite MIMO ring patch antenna for mobile communication system," *Progress In Electromagnetics Research B*, Vol. 25, 53–74, 2010.
8. Lin, S.-Y. and I.-H. Liu, "Small inverted-U loop antenna for MIMO applications," *Progress In Electromagnetics Research C*, Vol. 34, 69–84, 2013.
9. Sharawi, M. S., A. B. Numan, and D. N. Aloi, "Isolation improvement in a dual-band dual-element MIMO antenna system using capacitively loaded loops," *Progress In Electromagnetics Research*, Vol. 134, 247–266, 2013.
10. Chung, J.-Y., T. Yang, and J. Lee, "Low correlation MIMO antennas with negative group delay," *Progress In Electromagnetics Research C*, Vol. 22, 151–163, 2011.
11. Karimian, R., M. Soleimani, and S. M. Hashemi, "Tri-band four elements MIMO antenna system for WLAN and WiMAX application," *Journal of Electromagnetic Waves and Applications*, Vol. 26, Nos. 17–18, 2348–2357, 2012.
12. Zuo, S., Y.-Z. Yin, Z.-Y. Zhang, W.-J. Wu, and J.-J. Xie, "Eigenmode decoupling for MIMO loop-antenna based on 180° coupler," *Progress In Electromagnetics Research Letters*, Vol. 26, 11–20, 2011.
13. Cui, S., S. X. Gong, Y. Liu, W. Jiang, and Y. Guan, "Compact and low coupled monopole antennas for MIMO system applications," *Journal of Electromagnetic Waves and Applications*, Vol. 25, Nos. 5–6, 703–712, 2011.
14. Min, K.-S., M.-S. Kim, C.-K. Park, and M. D. Vu, "Design for PCS antenna based on WiBro-MIMO," *Progress In Electromagnetics Research Letters*, Vol. 1, 77–83, 2008.
15. Villanen, J., J. Ollikainen, O. Kivekas, and P. Vinikainen, "Coupling element based mobile terminal structures," *IEEE Transactions on Antennas and Propagation*, Vol. 54, No. 7, 2142–2153, 2010.
16. Vainikainen, P., J. Ollikainen, O. Kivekas, and I. Kelander, "Resonator-based analysis of the combination of mobile handset antenna and chassis," *IEEE Transactions on Antennas and Propagation*, Vol. 50, No. 10, 1433–1444, 2002.